Nanoscale

RSC Publishing

COMMUNICATION

View Article Online
View Journal | View Issue

Cite this: *Nanoscale*, 2013, **5**, 11620

Well-organized raspberry-like Ag@Cu bimetal nanoparticles for highly reliable and reproducible surface-enhanced Raman scattering†

Received 22nd July 2013
Accepted 21st September 2013

DOI: 10.1039/c3nr03363e

www.rsc.org/nanoscale

Jung-Pil Lee,[ab] Dongchang Chen,[c] Xiaxi Li,[a] Seungmin Yoo,[b] Lawrence A. Bottomley,[c] Mostafa A. El-Sayed,[c] Soojin Park*[b] and Meilin Liu*[a]

Surface-enhanced Raman scattering (SERS) is ideally suited for probing and mapping surface species and incipient phases on fuel cell electrodes because of its high sensitivity and surface-selectivity, potentially offering insights into the mechanisms of chemical and energy transformation processes. In particular, bimetal nanostructures of coinage metals (Au, Ag, and Cu) have attracted much attention as SERS-active agents due to their distinctive electromagnetic field enhancements originated from surface plasmon resonance. Here we report excellent SERS-active, raspberry-like nanostructures composed of a silver (Ag) nanoparticle core decorated with smaller copper (Cu) nanoparticles, which displayed enhanced and broadened UV-Vis absorption spectra. These unique Ag@Cu raspberry nanostructures enable us to use blue, green, and red light as the excitation laser source for surface-enhanced Raman spectroscopy (SERS) with a large enhancement factor (EF). A highly reliable SERS effect was demonstrated using Rhodamine 6G (R6G) molecules and a thin film of gadolinium doped ceria.

Surface-enhanced Raman scattering (SERS) is a powerful technique in surface science, electrochemistry, analytical chemistry, and biology due to its provision of vibrational fingerprint information of analytes with highly sensitive, surface-selective and non-destructive characterization.[1–5] There are two key mechanisms,[6–9] electromagnetic and chemical effects, mainly accepted for the enhancement of the SERS performance by several orders of magnitude after the first discovery of the phenomenon of enhanced Raman signals from adsorbed pyridine on roughened Ag surfaces in 1974 by Fleischmann.[10] According to the electromagnetic mechanism, the local electric field can be enhanced when surface plasma of the nanostructures is excited by incident light. Meanwhile, the chemical mechanism originates from charge transfer between SERS materials and adsorbed molecules.

Recently, intensive efforts have been devoted to developing new and reliable techniques based on the described mechanisms of SERS enhancement using coinage metal nanostructures, electrochemically roughened substrates, and lithographic patterns.[11–13] Nanoparticles of coinage metals, especially those composed of Au, Ag, or Cu, have attracted much interest due to their strong electromagnetic field enhancements produced from the optical response of plasmonic particles upon light irradiation.[3,11,14,15] Meanwhile, the new design of these functional materials is shifted toward more complex structures, including bimetal nanostructures in order to obtain further enhancement from materials chemistry.[16,17] Bimetal nanoparticles of alloy or core@shell structures often exhibit improved physical and chemical properties arising from the combination of different chemical compositions on the nanoscale that are impossible from one component.

However, synthesis of raspberry-like bimetal nanoparticles has not been reported, except for metal alloys[18,19] or core@shell[20–22] nanoparticles prepared by galvanic reaction.[23–25] Raspberry-like nanostructures of bimetals can feature a different chemical composition with higher surface area compared to the core@shell structures. Moreover, they can exhibit distinctive multi-functional properties compared to their single-component counterparts. From the viewpoints of practical SERS applications, the development of a facile synthetic route still remains a challenge for fabrication of reliable SERS-active materials with good reproducibility and uniformly high enhancement factor (EF).

To address this challenge, we have designed raspberry-like nanostructures, Cu-decorated Ag nanoparticles, for obtaining enhanced SERS performance with reproducible and uniform

[a]*School of Materials Science and Engineering, Center for Innovative Fuel Cell and Battery Technologies, Georgia Institute of Technology, 771 Ferst Drive, Atlanta, Georgia 30332-0245, USA. E-mail: meilin.liu@mse.gatech.edu; Fax: +1-404-894-9140; Tel: +1-404-894-6114*

[b]*Interdisciplinary School of Green Energy, Ulsan National Institute of Science and Technology (UNIST), Ulsan 689-798, Republic of Korea. E-mail: spark@unist.ac.kr; Fax: +82-52-217-2909; Tel: +82-52-217-2515*

[c]*School of Chemistry and Biochemistry, Georgia Institute of Technology, 901 Atlantic Drive, Atlanta, Georgia 30332-0400, United States*

† Electronic supplementary information (ESI) available. See DOI: 10.1039/c3nr03363e

response. The Ag nanoparticles with a narrow distribution in size and shape were prepared as seeds using a well-known polyol process.[17,21,26] The unusual raspberry nanostructures of Ag@Cu were produced after reduction of Cu precursors to Cu nanoparticles on the surface of Ag nanoparticles in the presence of poly(vinylpyrrolidone) (PVP) molecules and reducing agents. The raspberry-like Ag@Cu bimetal nanoparticles were systematically characterized by SEM, TEM, and UV-Vis spectroscopy. Furthermore, Rhodamine 6G (R6G) and gadolinium doped ceria thin films (GDC) were used as probes for SERS applications with the unique raspberry Ag@Cu structures compared to conventional core@shell structures.

Schematically depicted in Fig. 1a is the synthetic process for preparation of raspberry-like Ag@Cu bimetal nanoparticles by a stepwise reduction method. In the first step, Ag nanoparticles were obtained by a conventional polyol process, where ethylene glycol (EG) serves as a solvent as well as a reducing agent for reduction of Ag ions in the presence of PVP. Then, Cu precursors were reduced with hydrazine, leading to formation of Cu nanoparticles on the surface of the Ag nanoparticles (see the ESI† for details).

Fig. 1b–d show some typical morphologies of the raspberry-like Ag@Cu bimetal nanoparticles with uniform size and shape. As shown in Fig. 1b, all the Ag@Cu bimetal nanoparticles have well-organized raspberry-like forms with rough surfaces after decoration of the Cu nanoparticles on the surface of as-prepared Ag nanoparticles. The bright-field TEM image in Fig. 1c revealed that the products were composed of a variety of Cu nanoparticles grown on the surface of the Ag nanoparticles due to an electron density difference between Ag (dark) and Cu (grey). In particular, individual Cu nanoparticles with a diameter of ~5 nm are supported on the surface of each Ag nanoparticle, as can be seen from the high-magnification TEM image (Fig. 1d).

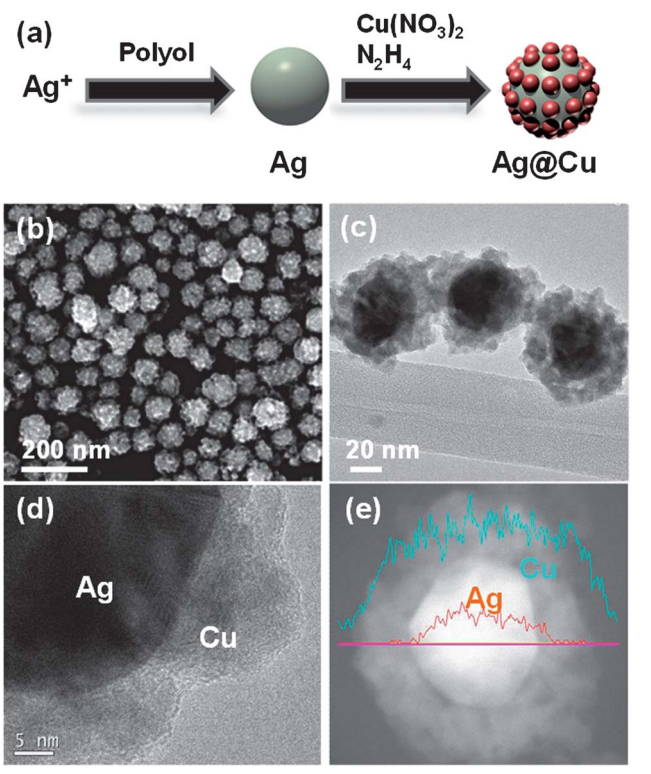

Fig. 1 (a) Scheme of fabrication of the raspberry-like Ag@Cu bimetal nanoparticles and structure analyses of the raspberry-like Ag@Cu bimetal nanoparticles. (b) SEM image of Ag@Cu particles loaded on a silicon substrate, TEM images with low (c) and high (d) magnification, and (e) EDX line-scanning profile across the representative Ag@Cu nanoraspberry bimetal nanoparticles.

Our synthetic routes to Ag@Cu raspberries are based on a modified polyol method. The reduction of metal precursors with polyol at high temperatures in the presence of polymeric capping agents has been regarded as a simple and versatile route to produce various kinds of metal particles.[17,21,26] In this study, spherical Ag nanoparticles (~45 nm) with a narrow size distribution (ESI, Fig. S1†) were first prepared by a polyol method, and subsequently, Cu nanoparticles were deposited on the Ag surface. PVP was added as a stabilizer to prevent Ag nanoparticle aggregation, and control the spatial locations of Cu ions on the surface of the Ag nanoparticles. Nucleation of the Cu nanoparticles was initiated on the surface of the Ag nanoparticles in the presence of PVP by reducing with hydrazine, and the well-defined raspberry-like Ag@Cu structures were obtained through further growth and self-assembly process of the individual Cu nanoparticles.[26]

Shown in Fig. 1e are some typical energy dispersive X-ray spectroscopy (EDX) line profiles that reveal the composition of the raspberry-like Ag@Cu bimetals. A single Ag nanoparticle (red signal) was located in the middle of the raspberry-like bimetal nanoparticle, while several distinct Cu nanoparticles (blue signal) were decorated in the outer regions. The corresponding atomic ratio of Ag to Cu obtained by element composition analysis was estimated to be ~2.6. In addition, HR-TEM and XRD analyses (Fig. S3†) indicated that Cu precursors were successfully converted to Cu nanoparticles (not to copper oxides) on the surface of the Ag nanoparticles.

UV-Vis spectroscopy was used to characterize the local surface plasmon resonance (LSPR) property of different nanostructured particles: spherical Ag, simple Ag@Cu core–shell structure, and Ag@Cu raspberry after spin-coating on cover glass. As is clearly seen in Fig. 2, the plasmonic peaks were shifted significantly with the nanostructures for these samples. The main absorption band of pure Ag nanoparticles (black dots) was located at 433 nm, consistent with their corresponding size and shape.[27] As a Cu shell is coated on the Ag core, the absorption band of the core@shell structure (blue triangle) was red shifted to 469 nm. It is well-known that the plasmon extinction maximum is shifted by changes in the shell thickness as well as its composition.[22,23] It is similarly observed in alloy systems with a range of compositions.[18]

Interestingly, isolated Cu nanoparticles on the Ag nanoparticles showed a new, broad plasmonic band in the range of 500–800 nm, covering the range corresponding to the Cu nanoparticles while retaining the typical absorption band of the Ag nanoparticles. Furthermore, the LSPR at 576 nm generated from the addition of the Cu nanoparticles increased gradually with the amount of Cu nanoparticles loaded onto the Ag particles (ESI, Fig. S4†). This is because the incident light will

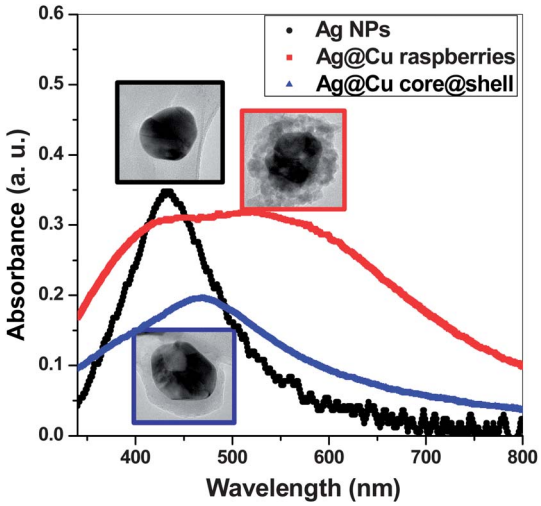

Fig. 2 Comparison of UV-Vis absorption spectra of the Ag nanoparticles and the Ag@Cu bimetal nanoparticles with a raspberry-like or a core@shell nanostructure.

interact not only with the Ag core portion of the raspberry-like Ag@Cu bimetal nanostructures but also with the isolated Cu nanoparticles, leading to broadening of the SPR peak (covering the wavelengths corresponding to both Ag and Cu nanoparticles). This phenomenon was not observed in core@shell and alloys type structures. It may be attributed to the distinctive behavior that the Cu nanoparticles on the individual Ag nanoparticles of the raspberry-like Ag@Cu bimetals were formed separately, resulting in their own SPR characteristics.[23,28] Moreover, the intensity of the Ag@Cu raspberries was higher than that of the Ag@Cu core@shell nanoparticles, because it was associated with higher surface area of the designed raspberries.

The raspberry-like Ag@Cu bimetal nanostructures were also characterized by SERS using three different excitation sources (488 nm for blue, 514 nm for green, and 633 nm for red laser) (see the ESI† for Raman characterization). The SERS effect of the Ag@Cu raspberries is evaluated using a commonly used dye molecule (R6G) in this study. Fig. 3a–c show the comparison results of the different nanostructures (raspberries and core@shell) of the Ag@Cu bimetals with R6G (5×10^{-9} M cm^{-2}) for the SERS. The Raman spectrum of R6G at a concentration of 5×10^{-9} M cm^{-2} is nearly featureless using all three excitation wavelengths, as shown in Fig. 3a–c. The Raman signal for R6G on the Ag@Cu nanoparticles was significantly enhanced. In particular, it was observed that the bands at 1648, 1574, 1505, and 1362 cm^{-1} are corresponding to C–C stretching in the xanthene plane for the typical characteristics of the R6G.[29]

It should be noted that SERS generated by noble nanoparticles depends strongly on particle aggregation.[9] Our samples were uniformly dispersed onto the substrates by a spin-coating method, as shown in Fig. 3d. The EF of the raspberry nanoparticles was estimated to be 600 and 220 under 514 nm and 488 nm laser excitation, respectively (see part 5 of the ESI†). In contrast, the EF of core@shell nanoparticles was calculated to be 140 under both laser excitations. Moreover, it is also noticed that the SERS effect of core@shell nanoparticles under the red laser is weak due to the fact that the plasmon band was far from 633 nm. In contrast, the SERS effect of Ag@Cu raspberries under the 633 nm is very substantial due to the new plasmon band between 500 and 800 nm. Under the red laser the EF of the raspberries is 7.3 times higher than that of core@shell nanostructures based on the intensity comparison, while there are no typical peaks in the case of pure R6G.

The EF based on the function of I_{normal} of R6G for the precise calculation (see the ESI† for the calculation of EF) with a high concentration of 5×10^{-7} M cm^{-2} which exhibited a clear Raman response is not higher than those of other reported SERS nanoparticles.[3,11,14] In addition, the Raman intensity enhanced by Ag@Cu raspberry nanoparticles is significantly higher than that of Ag@Cu core@shell nanoparticles at all incident laser wavelengths used in this study (Fig. 3a–c). The unique LSPR characteristics of the raspberry-like Ag@Cu bimetallic nanoparticles are reflected by the SERS effect at different excitation wavelengths. Under the blue laser (488 nm), both the raspberry like and core@shell nanoparticles provide a significant SERS effect, showing 220 and 140 times enhancement, respectively. When excited with the green laser (514 nm), the enhancement factor for the raspberry-like nanoparticles increased to 600, while it is still 140 for the core@shell nanoparticles. At red laser excitation (633 nm), the raspberry like nanoparticles still provide a prominent SERS effect, but the SERS effect of the core@shell particles is almost diminished (EF is difficult to calculate due to the low signal intensity of the normal Raman spectra). The unique enhancement effect of raspberry nanoparticles under the red laser is attributed to the LSPR peak at 500–600 nm, as a result of the exceptional architecture that allows both Ag and Cu to contribute to the SERS effect. Moreover, the Ag@Cu raspberry nanoparticles are proven to have better stability as shown in Fig. S6.† The Raman signal enhancement was well-preserved even after the samples were exposed to ambient air for 60 days.

It is noted that the signal intensity depends on the deposition method of R6G. The drop-coated R6G samples with the SERS nanoparticles appeared to have higher signal intensity than the spin coated samples, regardless of the type of nanoparticle (ESI Fig. S7†). The difference in SERS effect is attributed to the distribution of the SERS particles on the substrate, especially clustering of the particles resulted from the two methods. The SERS particles prepared by drop-casting were more clustered, thus producing stronger SERS effect than those from spin-coating. For a given deposition method, however, the SERS features were very reproducible as long as the coatings were uniform.

We extended raspberry-like Ag@Cu bimetal nanoparticles to other applications where they can act as SERS providers. In particular, shown in Fig. 4 is a typical application of SERS in the detection of Gd-doped ceria (GDC), which is commonly used to enhance carbon and sulphur tolerance as electrolytes of solid oxide fuel cells (SOFCs).[30,31] The SERS effect of the raspberry-like Ag@Cu bimetal nanoparticles was validated by loading them onto an annealed GDC thin film (~80 nm thick) deposited on a

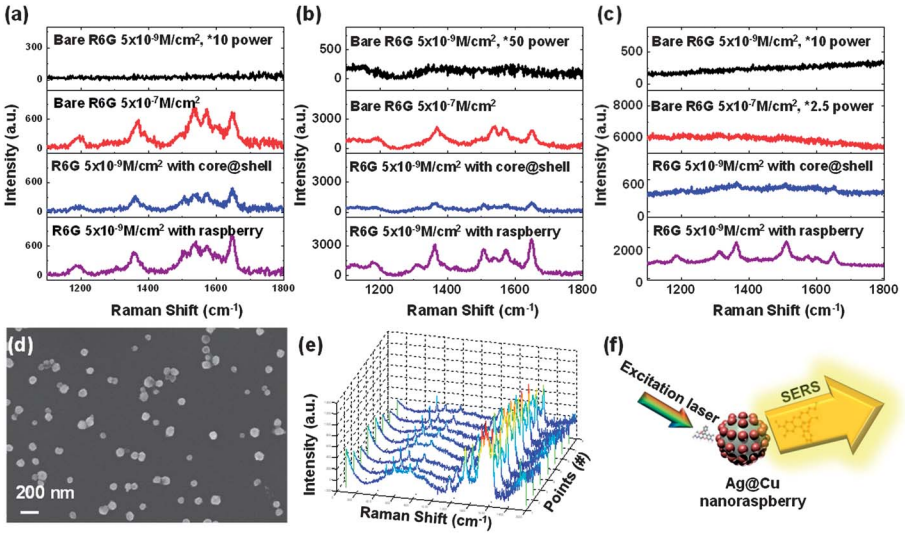

Fig. 3 Some typical SERS spectra of R6G with or without the raspberry-like and core@shell Ag@Cu bimetal nanoparticles using an excitation laser of wavelengths: (a) 488 nm, (b) 514 nm, and (c) 633 nm, (d) an SEM image of the raspberry-like Ag@Cu nanoparticles with the R6G (5×10^{-9} M cm^{-2}), (e) typical SERS spectra of R6G (5×10^{-9} M cm^{-2}) with Ag@Cu nanoraspberries collected at several points, and (f) scheme of SERS enhancement.

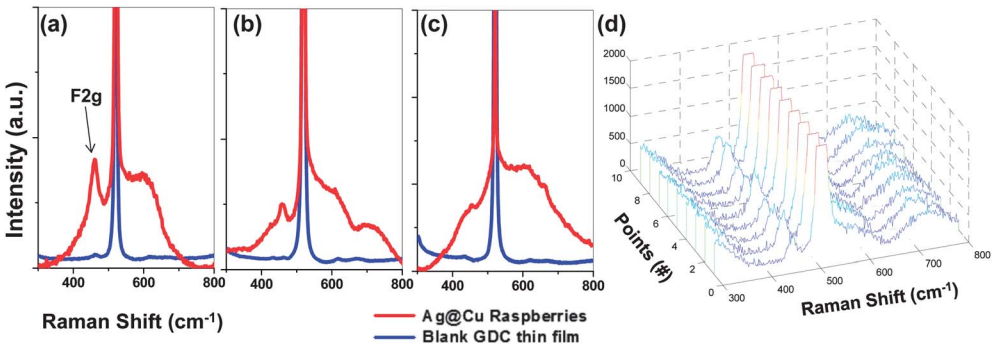

Fig. 4 Typical SERS spectra of a GDC thin film coated on a silicon substrate coated with the raspberry-like Ag@Cu bimetal nanoparticles using an excitation laser of wavelength: (a) 488 nm, (b) 514 nm, and (c) 633 nm, and (d) SERS spectra collected at several points under the 488 nm laser.

silicon wafer (ESI Fig. S8†). Three lasers with different wavelengths (488 nm, 514 nm, and 633 nm) were also used to inspect both the normal and surface enhanced Raman spectra of the GDC thin films. Under the 488 nm laser, the Ag@Cu nanoraspberry-loaded sample showed stronger signal than the blank GDC thin film, about 180 times enhancement in the F2g mode of the GDC thin film, which is located at around 460 cm^{-1}.[14] When excited with the 514 nm laser, the raspberry structured Ag@Cu nanoparticles provided 90 times enhancement to the F2g mode of GDC. This enhancement factor decreased slightly under the excitation of 633 nm laser to 50 times, further confirming the extraordinary SERS effect of Ag@Cu nanoraspberries under the 633 nm laser. It is well-known that the Raman activity of ceramic samples under 633 nm laser excitation is generally lower than that under 488 nm or 514 nm laser excitation.[14] The significant SERS improvement for Ag@Cu raspberry nanoparticles could potentially offer the convenience of Raman characterization of thin ceramic films under a wide range of excitation laser wavelengths. Furthermore, it is noted that the raspberry-like Ag@Cu bimetal nanostructures provide the analyzable SERS signals even though the Raman cross-section of the analytes is too low to be detected under a certain condition.

In summary, we have successfully fabricated raspberry-like bimetal nanostructures of uniform size and shape using a facile stepwise reduction process. Small Cu nanoparticles of tuneable size were individually deposited on the surface of the Ag nanoparticles in the presence of PVP during the reduction of Cu ions. It is shown that the finely organized Ag@Cu raspberries have surface plasmonic peaks in the range of 500–800 nm, covering those corresponding to both Ag and Cu nanoparticles. The peak intensities are also stronger than those of the core@shell structures of the Ag@Cu. As a result, a wide range of excitation laser wavelengths may be used for SERS characterization. Furthermore, the SERS enhancement is highly reproducible, as demonstrated by using R6G as a detecting molecule. Furthermore, the SERS-active nanostructures are also successfully used to study GDC as a typical ceramic material for the

solid oxide fuel cells. The bimetal nanoparticles with high surface area and distinct features may be used for other applications as well, including highly reliable and sensitive sensors.

Acknowledgements

This work was supported as part of the Heterogeneous Functional Materials (HeteroFoaM) Center, an Energy Frontier Research Center funded by the U.S. Department of Energy, Office of Science, Office of Basic Energy Sciences under the Award Number DE-SC0001061 and by the MSIP (NIPA-2013-H0301-13-1009) program.

Notes and references

1 M. J. Mulvihill, X. Y. Ling, J. Henzie and P. Yang, *J. Am. Chem. Soc.*, 2010, **132**, 268–274.
2 D.-K. Lim, K.-S. Jeon, J.-H. Hwang, H. Kim, S. Kwon, Y. D. Suh and J.-M. Nam, *Nat. Nanotechnol.*, 2011, **6**, 452–460.
3 S. M. Stranahan and K. A. Willets, *Nano Lett.*, 2010, **10**, 3777–3784.
4 X. Xu, K. Kim, H. Li and D. L. Fan, *Adv. Mater.*, 2012, **24**, 5457–5463.
5 B. Sharma, R. R. Frontiera, A.-I. Henry, E. Ringe and R. P. V. Duyne, *Mater. Today*, 2012, **15**, 16–25.
6 A. Otto, I. Mrozek, H. Grabhorn and W. Akemann, *J. Phys.: Condens. Matter*, 1992, **4**, 1143–1212.
7 M. Moskovits, *Rev. Mod. Phys.*, 1985, **57**, 783–826.
8 H. Xu, J. Aizpurua, M. Kall and P. Apell, *Phys. Rev. E: Stat. Phys., Plasmas, Fluids, Relat. Interdiscip. Top.*, 2000, **62**, 4318–4324.
9 A. Campion and P. Kambhampati, *Chem. Soc. Rev.*, 1998, **27**, 241–250.
10 M. Fleischmann, P. J. Hendra and A. J. McQuillan, *Chem. Phys. Lett.*, 1974, **26**, 163–166.
11 R. G. Freeman, K. C. Grabar, K. J. Allison, R. M. Bright, J. A. Davis, A. P. Guthrie, M. B. Hommer, M. A. Jackson, P. C. Smith, D. G. Walter and M. J. Natan, *Science*, 1995, **267**, 1629–1632.
12 S. Stewart and P. M. Fredericks, *Spectrochim. Acta, Part A*, 1999, **55**, 1615–1640.
13 Q. Yu, P. Guan, D. Qin, G. Golden and P. M. Wallace, *Nano Lett.*, 2008, **8**, 1923–1928.
14 X. Li, K. Blinn, Y. Fang, M. Liu, M. A. Mahmoud, S. Cheng, L. A. Bottomley, M. El-Sayed and M. Liu, *Phys. Chem. Chem. Phys.*, 2012, **14**, 5919–5923.
15 F. L. Yap, P. Thoniyot, S. Krishnan and S. Krishnamoorthy, *ACS Nano*, 2012, **6**, 2056–2070.
16 P. Cozzoli, T. Pellegrino and L. Manna, *Chem. Soc. Rev.*, 2006, **35**, 1195–1208.
17 D. Y. Kim, T. Yu, E. C. Cho, Y. Ma, O. O. Park and Y. Xia, *Angew. Chem., Int. Ed.*, 2011, **50**, 6328–6331.
18 M. B. Cortie and A. M. McDonagh, *Chem. Rev.*, 2011, **111**, 3713–3735.
19 J.-H. Liu, A.-Q. Wang, Y.-S. Chi, H.-P. Lin and C.-Y. Mou, *J. Phys. Chem. B*, 2005, **109**, 40–43.
20 M. Banerjee, S. Sharma, A. Chattopadhyay and S. S. Ghosh, *Nanoscale*, 2011, **3**, 5120–5125.
21 G. Park, D. Seo, J. Jung, S. Ryu and H. Song, *J. Phys. Chem. C*, 2011, **115**, 9417–9423.
22 M. M. Shahjamali, M. Bosman, S. Cao, X. Huang, S. Saadat, E. Martinsson, D. Aili, Y. Y. Tay, B. Liedberg, S. Chye, J. Loo, H. Zhang, F. Boey and C. Xue, *Adv. Funct. Mater.*, 2012, **22**, 849–854.
23 W. Xie, C. Herrmann, K. Kompe, M. Haase and S. Schlucker, *J. Am. Chem. Soc.*, 2011, **133**, 19302–19305.
24 G. D. Moon, S. Ko, Y. Min, J. Zeng, Y. Xia and U. Jeong, *Nano Today*, 2011, **6**, 186–203.
25 J. Chen, B. Wiley, J. McLellan, Y. Xiong, Z.-Y. Li and Y. Xia, *Nano Lett.*, 2005, **5**, 2058–2062.
26 Z. Li, V. Ravaine, S. Ravaine, P. Garrigue and A. Kuhn, *Adv. Funct. Mater.*, 2007, **17**, 618–622.
27 P.-Y. Silvert, R. H. Urbina and K. T. Elhsissen, *J. Mater. Chem.*, 1997, **7**, 293–299.
28 Z. Yi, X. Xu, X. Li, J. Luo, W. Wu, Y. Tang and Y. Yi, *Appl. Surf. Sci.*, 2011, **258**, 212–217.
29 C. Tian, B. Mao, E. Wang, Z. Kang, Y. Song, C. Wang and S. Li, *J. Phys. Chem. C*, 2007, **111**, 3651–3657.
30 R. C. Maher and L. F. Cohen, *J. Phys. Chem. A*, 2008, **112**, 1497–1501.
31 H. Kurokawa, T. Z. Sholklapper, C. P. Jacobson, L. C. De Jonghe and S. J. Visco, *Electrochem. Solid-State Lett.*, 2007, **10**, B135–B138.

